Design considerations for a hybrid wind-wave platform under energy-maximising control

Maria Luisa Celesti, Bruno Paduano, Yerai Peña-Sanchez, Edoardo Pasta, Nicolás Faedo and John V. Ringwood

Abstract—**The environmental impact of emissions of fossil fuels and their rising prices, together with countries' commitment to mitigate the effect of the alarming and rapid climate changes, have been a crucial thrust to investigate new solutions to exploit renewable energies for efficient and effective energy supply. Offshore wind-wave hybrid platforms have been proposed to produce higher-quality power at a lower cost, by exploiting the existing synergies between these two technologies. The aim of this study is to investigate the effects of structural (geometric) design changes on the dynamics of a hybrid wind-wave platform under energy-maximising control for the wave conversion system. In particular, the device considered is a semi-submersible platform with an incorporated flap-type WEC, analysed both from a closed-loop and open-loop perspectives with a control system designed to maximise the energy produced by the WEC. Design changes on the wind-wave conversion platform are performed in terms of flap dimensions, starting from a suitably defined nominal geometry. The corresponding dynamical analysis is conducted by both increasing and decreasing the flap draft with respect to the nominal case, to investigate the effect of different structures on the interactions between WEC and platform. A frequency-domain analysis of the overall input/output (velocity) system is presented, highlighting the situations that can enhance the potential of both devices and exploit their synergies.**

Index Terms—**Combined wind-wave, design changes, floating offshore platform, wave energy.**

I. Introduction

THE necessity of reducing the carbon footprint related to energy supply, led to the exploitation of renewable energy sources. Among these, wind and wave, having a complementary distribution worldwide, can be effectively powerful candidate energy sources towards a full transition to renewable energies [1]. Therefore, it is crucial to have technologies capable of efficiently harnessing these sources. Onshore wind turbines are already highly mature technologies, presenting however their own limitations, particularly with respect to availability of suitable lands. Nowadays, there is a transition towards offshore wind systems: although still at an early stage of development, these technologies can potentially exploit wind power in locations with higher energy density, reducing some of the on-shore wind farm-related problems, such as noise pollution and visual impact [2], [3]. Combining off-shore wind technology with other energy conversion systems, such as wave energy converters (WECs), has the advantage of exploiting both wind and wave sources, hence having the prospect of a more smooth and reliable power production due to the higher predictability of the wave source and the low correlation between the two resources [4], [5]. In other words, their aggregation and combination can reduce the overall variability of the power extraction process. Furthermore, these hybrid platforms, sharing the same foundation systems, infrastructures and grid connections, can have the advantage of reducing the cost of operation and maintenance [6], [7]. The integration of WECs in a floating off-shore wind turbine can enhance dynamic stability by using the WEC to dampen the platform motion and increase the power production of the overall system compared to their standalone counterpart [8].

For the WEC system, adequate control technology is crucial to ensure maximum energy extraction from ocean waves, improving reliability and reducing the associated levelised cost of energy (LCOE) [9]. Moreover, an appropriate design is fundamental for the overall system performance [10]. In fact, by changing the associated geometry, different dynamic behaviour occurs in the system, potentially resulting in more suitable designs, depending on the specific sea-state conditions, as clarified in Section IV.

Motivated by the relevance and overall effect of both suitable control technology and structural (geometric) changes to the WEC system, the aim of this study is to investigate systematically the effect of different WEC designs in a combined wind-wave conversion platform under energy-maximising control. The controller is designed based on the principle of *impedance-matching* [11], in terms of a reactive, *i.e.* proportional-integral (PI), controller structure synthesised according to each specific sea-state condition under analysis.

This paper is organised in the following sections. Section II provides a description of the case study presented within this paper. Section III briefly recalls the fundamentals of hydrodynamic modelling of floating structures and the associated energy-maximising control design procedure. Finally, Section IV illustrates the main numerical results obtained within this study, while Section V offers an overview of the conclusions.

M. L. Celesti, B. Paduano, E. Pasta, and N. Faedo are with the Marine Offshore Renewable Energy Lab, Politecnico di Torino, Turin, Italy (Corresponding author: M. L. Celesti - maria.celesti@polito.it).

Y. Peña-Sanchez is with the Department of Mathematics, Euskal Herriko Unibertsitatea, Bilbao, Basque Country.

J. V. Ringwood is with the Centre for Ocean Energy Research, Maynooth University, Maynooth, Ireland.

Digital Object Identifier:
https://doi.org/10.36688/ewtec-2023-590

II. Case study

In this study, one of the most wide-spread wind-wave hybrid concepts has been chosen: the so-called *WindWaveFloat* system [12]. This hybrid platform exploiting both wind and wave resources, sharing support structures and infrastructures, can potentially offer a significant contribution towards the reduction of emissions and the mitigation of the effects of climate change. The device is constituted of a three-column semi-submersible platform with a standard horizontal-axis wind turbine (NREL 5 MW) at the top of a tower, sitting on the rear column, and a rectangular flap-type WEC mounted on the main beam. The overall system is based on the WindWaveFloat for the platform structure, and the *Oyster* device for the WEC (see [13]). Furthermore, note that the selected wind turbine can be considered to be standard, and has been the subject of a number of studies concerning wind-wave hybrid platforms [14]–[17]. Within this study, although the wind turbine has been effectively considered within the calculation of the floating structure response the dynamical analyses are conducted considering the overall platform directly, hence using platform pitching motion as a proxy for turbine pitching movement.

TABLE I
Main parameters of the wind-wave structure with respect to the still water level.

Flap width	1.5 [m]
Flap length	15 [m]
Nominal flap draft	6.5 [m]
Platform cylinder radius	5 [m]
Platform draft	15 [m]

Table I summarises the main parameters associated with the considered wind-wave platform, while Figure 1 provides a schematic of the corresponding geometry, considering only the portion in which the flap is located, whereas the whole system is reported in Figure 2. In particular, the black solid line indicates the nominal geometry, while dashed lines are used to denote the largest and smallest draft considered within this study for the flap system.

In fact, the effects of design changes are evaluated by increasing and decreasing flap dimensions in terms of its depth. As reported in Table II, a fixed step of 1 [m] is taken between each different design.

TABLE II
Design changes in WEC dimensions.

Flap draft				
4.5 [m]	5.5 [m]	6.5 [m] (nominal)	7.5 [m]	8.5 [m]

III. Modelling and control

Within this section, modelling fundamentals, in terms of linear potential flow theory, and the control technique applied to the floating structure, are briefly recalled. As it is standard within the control/estimation literature, the hydrodynamics of the combined platform are described by means of linear equations leveraging potential flow theory, with the aim of deriving

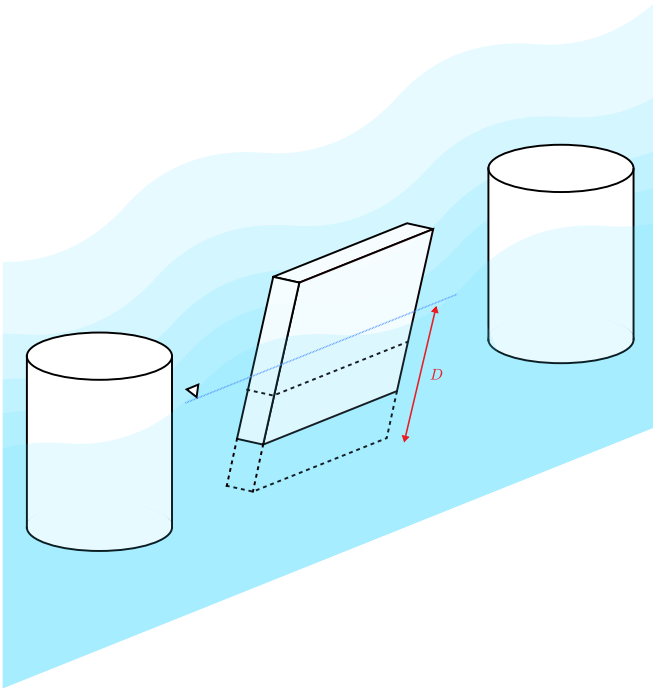

Fig. 1. Design changes of the WEC in terms of the draft, D.

a computationally and analytically tractable representation for the overall system (*i.e.* a control-oriented model). Therefore the equation of motion for the floating body can be written in terms of Newton's second law as follows:

$$M\ddot{x}(t) = f_{ex}(t) + f_{re}(t) + f_r(t) - u_t(t), \qquad (1)$$

where M is the generalised inertia-mass matrix of the structure, x denotes the displacement vector associated with the floating system (in all considered degrees-of-freedom (DoFs)), f_{ex} the wave excitation force (*i.e.* the torque exerted on the wetted surface of the device by the incoming wave field), and f_{re} the hydrostatic restoring force that, under linear potential theory, is given by $f_{re} = s_h z$, where s_h represents the so-called hydrostatic stiffness. Furthermore, f_r indicates the radiation force (force of the waves generated by the oscillatory motion of the body), which can be modelled using the well-known Cummins' equation [18], and can be numerically characterised using boundary element solvers. In particular, for the computation of the hydrodynamic coefficients associated with the system, the boundary element method (BEM) solver OrcaWave [19] is used, leveraging the mesh of the system reported in Figure 2.

The radiation force can be expressed by the following equation:

$$f_r = -m_\infty \ddot{x} - k_r * \dot{x}, \qquad (2)$$

where m_∞ is the so-called added mass at infinity frequency, and k_r is the radiation impulse response function, which fully characterises an associated linear time-invariant operator. Finally, u_t is the control input applied through the power take-off (PTO) system of the WEC device, designed and synthesised, within this paper, following the so-called impedance-matching

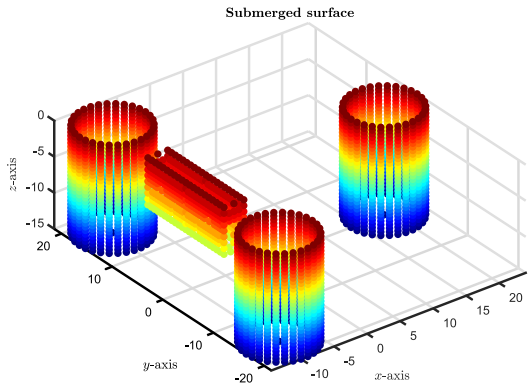

Fig. 2. Mesh of the combined wind-wave system used for the computation of the hydrodynamic coefficients.

principle [20]. According to this theory, maximisation of converted energy can be achieved by adjusting, via suitable control, the PTO impedance to match the complex-conjugate of the impedance associated with the WEC, as further discussed in Section III-A.

Let $v = \dot{x}$. The equation of motion in the frequency-domain, after a direct application of Fourier transform[1], can be written as

$$\jmath\omega(M + m_\infty)V = -K_r V - \frac{s_h}{\jmath\omega}V + F_{ex} - U_t, \quad (3)$$

from which the input/output map $F_{ex} \mapsto V$ can be written in terms of the following expression:

$$\begin{aligned} V(\jmath\omega) &= \left[(M + m_\infty)\jmath\omega + K_r + \frac{s_h}{\jmath\omega}\right]^{-1}(F_{ex} - U_t) \\ &= G(F_{ex} - U_t), \end{aligned} \quad (4)$$

where G denotes the frequency-response function associated with the corresponding I/O map.

The device considered within this study, presented in Section II, is described in terms of 2 DoFs, *i.e.* pitch of both platform and WEC. Energy extraction for the WEC device effectively happens with the PTO system sitting on the corresponding pitch axis, and hence the system can be described, exploiting the relation posed in (4) in an input/output (I/O) form as follows:

$$\begin{bmatrix} V_p \\ V_f \end{bmatrix} = \begin{bmatrix} G_{11} & G_{12} \\ G_{21} & G_{22} \end{bmatrix} \begin{bmatrix} F_p \\ F_f - U \end{bmatrix}, \quad (5)$$

in which $\{V_p, V_f\}$ and $\{F_p, F_f\}$ denote the velocities and torques, respectively, of both platform and flap, and hence $G : \mathbb{C} \to \mathbb{C}^{2\times 2}$, $s \mapsto G(s)$, is the mapping characterising the system. In particular, $\{G_{11}, G_{12}\}$ describes the relation between torque and pitch velocity for the platform, whereas $\{G_{21}, G_{22}\}$ defines the response for the WEC pitching motion. Note that U in (5) refers to the control action applied via the PTO associated with the WEC system.

A. Control design and synthesis

The technique utilised to design and synthesise the controller is shortly described within this section. The control input u has to maximise the converted energy for the WEC, and it is based on the impedance-matching principle [20]. The main objective of WEC control is to enable optimal energy capture from ocean waves via the associated PTO system. However, the energy available in ocean waves varies over time due to changes in wave height, wave period, and wave direction. Therefore, WECs must be able to adjust their motion in response to the changing wave conditions to capture as much energy as possible.

In particular, the control input u is designed and synthesised to match the complex-conjugate of the mechanical impedance characterising the WEC. The optimal control condition, written in the frequency domain, is the following:

$$U^{\text{opt}} = I_u V_f, \quad (6)$$

with the so-called control 'load' I_u defined as

$$I_u(\jmath\omega) = I^*(\jmath\omega) = \frac{1}{G_{22}^*(\jmath\omega)}, \quad (7)$$

where I^* indicates the complex-conjugate of the equivalent intrinsic impedance associated with the WEC (see [20] for further detail on the definition of the intrinsic impedance in the multi-DoF case).

Due to the nature of the complex-conjugate operator, the optimal condition can not be physically implemented, and hence an approximation is required (see [20]). Such an approximating system can be practically achieved via parametric controllers. In particular, a well-established structure among the WEC literature has been implemented, *i.e.* a proportional-intergal (PI) controller, often referred to as 'reactive' controller:

$$K_{PI}(s) = \theta_1 + \frac{\theta_2}{s}. \quad (8)$$

The controller, implemented within this study, is of a feedback nature, as reported in Figure 3.

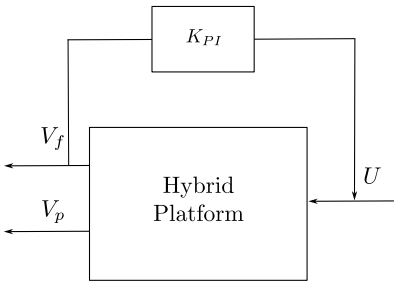

Fig. 3. Feedback control structure implemented for the device.

Unlike standard (tracking and regulation) control applications, the parameters associated with (8) are chosen to interpolate the optimal frequency-domain condition derived via impedance-matching, *i.e.* equations (6), (7). In particular, depending on the incoming wave, with the corresponding frequency ω_i, there are different θ_1 and θ_2 interpolating the optimal control impedance I_u in (7), *i.e.* leading to the interpolation condition $K_{PI}(\jmath\omega_i) = I_u(\jmath\omega_i)$, and computed as follows:

$$\theta_1 = \Re(I_u(\jmath\omega_i)), \qquad \theta_2 = -\omega_p \Im(I_u(\jmath\omega_i)) \quad (9)$$

[1]Given a time-domain function f, its Laplace/Fourier transforms are denoted as F, where the use of Laplace or Fourier is always clear from the context.

In other words, there is an optimal PI control structure for each specific sea-state. This is specifically considered within our study, where the parameters $\{\theta_1, \theta_2\}$ are effectively synthesised for each operating condition. In particular, considering the case of irregular waves, the interpolation point can be chosen according to the peak frequency $\omega_p = 2\pi/T_p = \omega_i$, where T_p is the peak period of the spectral density function characterising the sea-state.

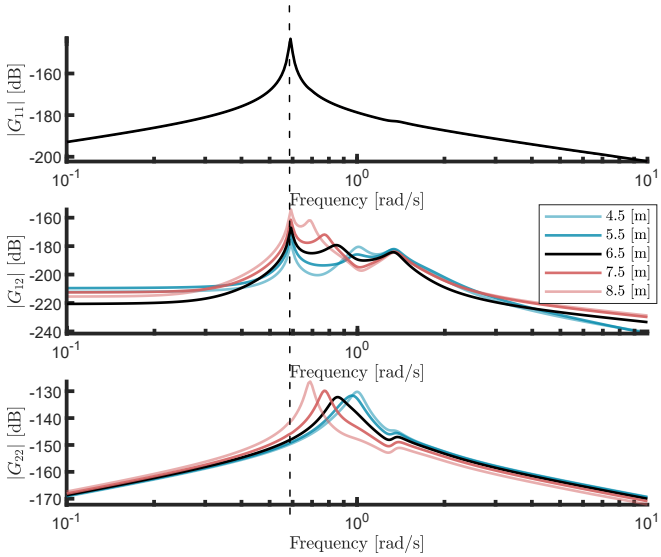

Fig. 4. Design changes effect on the magnitude of the frequency response of the open-loop system.

IV. Numerical results

In this section, the main numerical results obtained within this study are reported. Firstly, the open-loop case is considered, hence analysing only the effect of the design changes in the flap geometry in the absence of control. Then, different geometries are considered coupled with the energy-maximising controller previously evaluated, *i.e.* in a closed-loop sense.

To begin with the analysis presented within this study, the Bode diagram, offering magnitude and phase, presents the frequency response associated with the transfer function of the overall system, *i.e.* Equation (5). The nominal geometry case is reported using a black line, while, using blue and red-colour scales are shown, respectively, decreased and increased flap dimensions with respect to the nominal case. It is immediately evident that geometry changes directly result in a different resonant frequency of the flap ω_f: in fact, increasing the flap dimension, as can be clearly seen in Figure 4, leads to a shift of the magnitude peak to the left (*i.e.* the low-frequency range). Analogously, decreasing in size moves the flap resonance frequency accordingly, though towards the high-frequency end of the spectrum. When increasing the dimension, ω_f becomes closer to the platform resonance, ω_p, hence amplifying the level of interaction between the two subsystems (*i.e.* flap and platform), which consequently results in an increase of the magnitude associated with the mapping relative to this coupling, *i.e.* G_{12}.

To further expand the findings presented in Figure 4, effect of geometry changes can be evaluated in terms of the ratio of the root mean square value of flap and platform pitch position, in controlled (closed-loop) and uncontrolled (open-loop) conditions. The considered input waves are generated in terms of a JONSWAP [21] spectrum, with peak frequencies in the set $\mathcal{W} = [0.8\omega_f, 1.2\omega_f]$, where ω_f changes accordingly with the dimension of the flap. Controlled conditions are evaluated with a design based on the PI energy-maximising control, as specified in Section III, with parameters synthesised according to the specific sea-state. In Figure 5 (middle) the nominal geometry case is reported, while left- and right-hand-side plots illustrate the results concerning the smallest and largest WEC depth considered within this study, respectively.

As mentioned immediately above, an increase of flap dimension brings the overall flap resonance frequency closer to the platform one. Having more proximate dynamics translates into a stronger interaction between the two devices. In this scenario, the WEC potential to affect the platform displacement is hence enhanced. In fact, when considering the flap with a 4.5 [m] depth, the ratio for the platform is ≈ 1 for the whole range of input frequencies considered, even though the flap movement is changing considerably. When increasing the flap depth, instead, the platform position ratio is no longer around 1, particularly for sea-states with peak frequency far from ω_f. This directly implies that flaps with larger dimensions can highly affect the platform behaviour also when under control conditions.

Another important aspect to evaluate is the order of magnitude of the force necessary to reach the WEC control objective when changing the geometry. Figure 6 reports the root mean square value of the control torque as a function of the flap draft. This value is estimated considering as input wave frequency the endpoints of the set $\mathcal{W}$, *i.e.* when ω_i equals $0.8\omega_f$ and $1.2\omega_f$, respectively. Note that the results are a direct expansion of the findings reported in Figure 4: in fact, as reported in (6) and (7), the optimal control condition is defined in terms of the inverse of G_{22}^*, and, hence, considering an input frequency ω_i with higher magnitude leads to smaller values of the control U. In both cases considered, the action necessary to reach energy-maximisation for the flap with 8.5 [m] draft is larger than the one required for smaller depths.

V. Conclusions

The present study investigates the impact of WEC design changes in a hybrid wind-wave conversion platform under energy-maximising control. The findings clearly indicate that diverse flap geometries lead to differences in terms of flap-platform interaction and control force required to reach energy-maximisation. These differences lead to more advantageous designs depending on the application, *i.e.* to a more suitable design capable of better exploiting the specific wave condition. Furthermore, the consequences of having a higher interaction between WEC and platform can be desirable when the former is used in the hybrid device

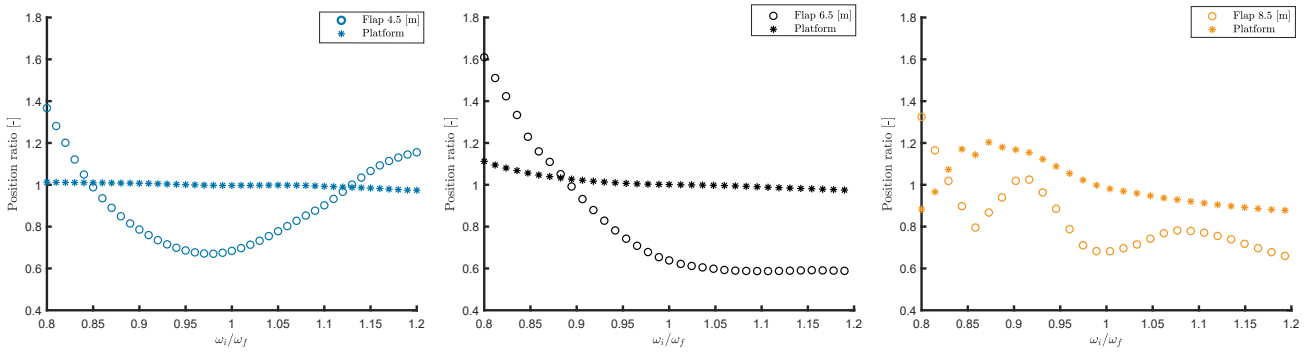

Fig. 5. Ratio of the root mean square value of flap and platform pitch position in controlled/uncontrolled conditions changing geometry. a) decrease of the draft, b) nominal geometry, c) increase of the draft.

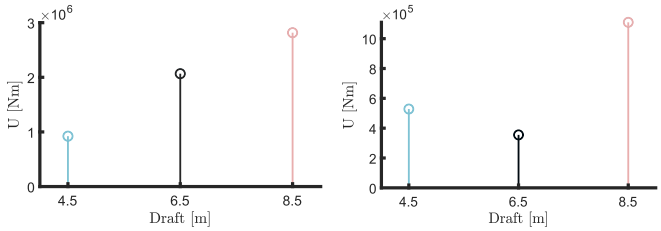

Fig. 6. Root mean square value of the control torque at different draft considering different ω_i.

with stabilisation purposes. On the other hand, if the WEC control objective is energy-maximisation, which often leads to large amplitude motion, distant dynamics between flap and platform can be potentially convenient. In fact, a lower interaction translates into the possibility of free movement for the WEC in a wider range of frequencies, without strongly affecting the platform position. As previously highlighted, higher interactions are a direct consequence of the vicinity between platform and flap resonances. This proximity can be reached both by increasing WEC dimensions or by decreasing the dimensions of the platform. A deeper investigation will aim at highlighting the economic convenience of the latter option. Further analyses will take into account the WEC influence on wind turbine efficiency and the effect of specific wind controllers. Finally, also the difference in terms of required control actions, strongly depending both on the designs and on the incoming waves, can be positively exploited to identify the most beneficial and economically effective concept to operate in a specific sea-state.

REFERENCES

[1] A. M. Cornett, "A global wave energy resource assessment," in *The Eighteenth international offshore and polar engineering conference*. OnePetro, 2008.

[2] M. Bilgili, A. Yasar, and E. Simsek, "Offshore wind power development in europe and its comparison with onshore counterpart," *Renewable and Sustainable Energy Reviews*, vol. 15, no. 2, pp. 905–915, 2011.

[3] A. S. Darwish and R. Al-Dabbagh, "Wind energy state of the art: present and future technology advancements," *Renewable Energy and Environmental Sustainability*, vol. 5, p. 7, 2020.

[4] F. Fusco and J. V. Ringwood, "Robust control of wave energy converters," in *2014 IEEE Conference on Control Applications (CCA)*. IEEE, 2014, pp. 292–297.

[5] C. Perez and G. Iglesias, "Integration of wave energy converters and offshore windmills," in *http://www. icoe-conference. com*, 2012.

[6] D. M. Skene, N. Sergiienko, B. Ding, and B. Cazzolato, "The prospect of combining a point absorber wave energy converter with a floating offshore wind turbine," *Energies*, vol. 14, no. 21, p. 7385, 2021.

[7] S. Saeidtehrani, T. Fazeres-Ferradosa, P. Rosa-Santos, and F. Taveira-Pinto, "Review on floating wave-wind energy converter plants: Nonlinear dynamic assessment tools," *Sustainable Energy Technologies and Assessments*, vol. 54, p. 102753, 2022.

[8] E. Petracca, E. Faraggiana, A. Ghigo, M. Sirigu, G. Bracco, and G. Mattiazzo, "Design and techno-economic analysis of a novel hybrid offshore wind and wave energy system," *Energies*, vol. 15, no. 8, p. 2739, 2022.

[9] J. V. Ringwood, G. Bacelli, and F. Fusco, "Energy-maximizing control of wave-energy converters: The development of control system technology to optimize their operation," *IEEE control systems magazine*, vol. 34, no. 5, pp. 30–55, 2014.

[10] J. van Rij, Y.-H. Yu, K. Edwards, and M. Mekhiche, "Ocean power technology design optimization," *International Journal of Marine Energy*, vol. 20, pp. 97–108, 2017.

[11] N. Faedo, E. Pasta, F. Carapellese, V. Orlando, D. Pizzirusso, D. Basile, and S. A. Sirigu, "Energy-maximising experimental control synthesis via impedance-matching for a multi degree-of-freedom wave energy converter," *IFAC-PapersOnLine*, vol. 55, no. 31, pp. 345–350, 2022.

[12] A. Weinstein, D. Roddier, and K. Banister, "Windwavefloat (wwf): Final scientific report," Principle Power Inc., United States, Tech. Rep., 2012.

[13] T. Whittaker, D. Collier, M. Folley, M. Osterried, A. Henry, and M. Crowley, "The development of oyster—a shallow water surging wave energy converter," in *Proceedings of the 7th European wave and tidal energy conference*, 2007, pp. 11–14.

[14] N. Ren, Z. Ma, B. Shan, D. Ning, and J. Ou, "Experimental and numerical study of dynamic responses of a new combined tlp type floating wind turbine and a wave energy converter under operational conditions," *Renewable Energy*, vol. 151, pp. 966–974, 2020.

[15] N. Ren, Z. Ma, T. Fan, G. Zhai, and J. Ou, "Experimental and numerical study of hydrodynamic responses of a new combined monopile wind turbine and a heave-type wave energy converter under typical operational conditions," *Ocean engineering*, vol. 159, pp. 1–8, 2018.

[16] S. Jovašević, M. R. S. Mohammadi, C. Rebelo, M. Pavlović, and M. Veljković, "New lattice-tubular tower for onshore wec–part 1: Structural optimization," *Procedia engineering*, vol. 199, pp. 3236–3241, 2017.

[17] B. Fenu, V. Attanasio, P. Casalone, R. Novo, G. Cervelli, M. Bonfanti, S. A. Sirigu, G. Bracco, and G. Mattiazzo, "Analysis of a gyroscopic-stabilized floating offshore hybrid wind-wave platform," *Journal of Marine Science and Engineering*, vol. 8, no. 6, p. 439, 2020.

[18] W. Cummins, "The impulse response function and ship motions," David Taylor Model Basin Washington DC, Tech. Rep., 1962.

[19] Orcina, "OrcaFlex - Documentation, 10.1b Edition," Tech. Rep., 2020. [Online]. Available: https://www.orcina.com/SoftwareProducts/OrcaFlex/Documentation/

[20] N. Faedo, F. Carapellese, E. Pasta, and G. Mattiazzo, "On the principle of impedance-matching for underactuated wave energy harvesting systems," *Applied Ocean Research*, vol. 118, p. 102958, 2022.

[21] K. Hasselmann *et al.*, "Measurements of wind-wave growth and swell decay during the joint north sea wave project (jonswap)." *Ergaenzungsheft zur Deutschen Hydrographischen Zeitschrift, Reihe A*, 1973.